

Received 19 March 2018; revised 3 June 2018; accepted 20 June 2018. Date of publication 31 October 2018; date of current version 1 March 2019. The review of this paper was arranged by Editor S. Vaziri.

Digital Object Identifier 10.1109/JEDS.2018.2854633

Low-Temperature MoS₂ Film Formation Using Sputtering and H₂S Annealing

JUN'ICHI SHIMIZU¹, TAKUMI OHASHI¹, KENTARO MATSUURA¹, IRIYA MUNETA¹ (Member, IEEE), KUNIYUKI KAKUSHIMA¹ (Member, IEEE), KAZUO TSUTSUI¹ (Senior Member, IEEE), NOBUYUKI IKARASHI², AND HITOSHI WAKABAYASHI¹ (Member, IEEE)

¹ Tokyo Institute of Technology, Yokohama 226-8502, Japan

² Nagoya University, Nagoya 464-8603, Japan

CORRESPONDING AUTHOR: H. WAKABAYASHI (e-mail: wakabayashi.h.ab@m.titech.ac.jp)

This work was supported in part by JST CREST under Grant JPMJCR16F4, in part by JST Center of Innovation Program, in part by JSPS KAKENHI under Grant 26105014, and in part by the Nagoya University.

ABSTRACT Low-carrier density and high-crystallinity molybdenum disulfide (MoS₂) films were fabricated by low-temperature and clean process based on a UHV RF sputtering system. This paper focuses on improving crystallinity and reducing the number of sulfur defects of sputtered-MoS₂ film. We have fabricated MoS₂ films at lower than 400°C using the sputtering and H₂S post-deposition annealing processes. Consequently, MoS₂ films with high crystallinity and appropriate S/Mo ratio were obtained. Eventually, a low carrier density of $3.5 \times 10^{17} \text{ cm}^{-3}$ and the Hall-effect mobility of $12 \text{ cm}^2\text{V}^{-1}\text{s}^{-1}$ were achieved.

INDEX TERMS Transition metal di-chalcogenide, TMDC, molybdenum disulfide (MoS₂), UHV RF sputtering, H₂S annealing.

I. INTRODUCTION

Molybdenum di-sulfide (MoS₂) has attracted considerable attention because of its remarkable electrical and mechanical properties. Examples of such properties include a bandgap of 1.2–1.8 eV [1], [2] and high mobility up to $400 \text{ cm}^2\text{V}^{-1}\text{s}^{-1}$ even in atomically thin film [3]–[5] in which the mobility seriously decreases in the case of bulk materials such as silicon and InGaAs [6]–[8].

Transfer-type film formation processes such as Scotch-tape and liquid exfoliation are widely adopted [3]–[5], [9]. The exfoliation has an advantage in which it easily enables the formation of a thin MoS₂ film and achieves high mobility in the MoS₂ film up to $400 \text{ cm}^2\text{V}^{-1}\text{s}^{-1}$. However, the exfoliated-MoS₂ film has a high carrier density of 10^{20} cm^{-3} caused by pollutions such as carbon and alkali metals, and also a difficulty in forming the large-area MoS₂ film, which is necessary for industrial applications.

To overcome these problems, bottom-up processes such as chemical vapor deposition (CVD), atomic layer deposition (ALD), pulse laser deposition (PLD) and sputtering are required. The CVD, in which MoO₃, sulfur powder,

and hydrogen sulfide (H₂S) are commonly used as precursors, is widely used because it allows us the synthesis of high-quality MoS₂ film on a sapphire substrate [10]–[16]. Although large-grain and high-quality MoS₂ film can be obtained, the deposition temperature is commonly high at 600°C or more which is not appropriate for application such as 3D-monolithic ICs which require low thermal budget [17], [18]. Thus, reducing the formation temperature is important for maintaining high crystallinity of the channel material.

The ALD has been investigated because of the possibilities such as low-temperature process, large-scale deposition and high controllability of film thickness. It has been reported that MoS₂ films were able to be formed by using Mo(CO)₆ [19]–[21], MoCl₅ [22]–[25] or Mo(thd)₃ [26] with H₂S gas. However, these processes are simultaneously associated with some disadvantages such as the high temperature of post-deposition annealing, carbon contamination, and low-crystallinity of MoS₂ film.

On the other hand, a sputtering process is considered to allow us a low-temperature, carbon-free, and large-scale film

formation. Recently, the reactive sputtering with a molybdenum (Mo) target and sulfur (S) powder was used to form MoS₂ thin film as a semiconductor, although it is a high-temperature process at up to 700°C [27]. Thus, an alternative sputtering method, which can be used to form MoS₂ films at low temperature, is required. Instead of the Mo target, MoS₂ target is selected to reduce temperature on large area with less impurities [28]–[36]. However, it was found that the carrier density of sputtered-MoS₂ film is comparatively high as 10¹⁸ cm⁻³ approximately due to sulfur defects which have been discussed as n-type dopants in the case of the MoS₂ film because sulfur defects generate states with an energy level of 0.2 eV near the conduction band minimum in monolayer MoS₂ film [37]. The film prepared by sulfur compensation process using sulfur powder annealing has high crystallinity and low carrier density of 10¹⁶ cm⁻³, approximately [32]. However, the annealing temperature up to 700°C is comparatively higher than we had expected. In order to reduce annealing temperature, we used H₂S gas because of its high reactivity.

In this study, we conducted low-temperature H₂S annealing on sputtered-MoS₂ film to achieve high crystallinity MoS₂ film resulting in the low carrier density.

II. EXPERIMENTAL METHODS

A SiO₂/Si substrate of 2 cm × 2 cm was cleaned by a wet process using piranha solution. Then, a MoS₂ film of 5-nm thickness was deposited on the substrate by RF sputtering system with four-inch-diameter sample stage. The conditions were: RF power of 50 W; distance between the target and substrate of 150 mm; substrate temperature at 400°C; argon (Ar) flow of 7.0 sccm; and partial pressure under 0.55 Pa. Then, the MoS₂ film was annealed in Ar gas with 1% H₂S gas instead of forming gas (F.G.: 3% H₂ in N₂) under 10k-300 Pa at up to 400°C using hot-wall annealing system as an *ex-situ* process. Raman spectroscopy with a laser wavelength of 488 nm, X-ray photoelectron spectroscopy (XPS) using an Al K α X-ray source and scanning transmission electron microscopy (STEM) were performed. As electrical characteristics, the Hall effect was measured in centimeter-level MoS₂ film with silver past by using ResiTest8400 of TOYO Corporation.

III. RESULTS AND DISCUSSION

Figs. 1 and 2 show the Raman spectra for as-sputtered and annealed MoS₂ films depending on the gas/pressure and annealing temperature, respectively. In these figures, H₂S annealing reduces the intensity of MoO₃ peak over 300°C as compared with as-sputtered and F.G.-annealed MoS₂ films. Although it has been reported that sulfur vacancies cause tensile strain in MoS₂ film formed by exfoliation process [39], E_{2g}¹ peaks with H₂S annealing process shift to higher wavenumber direction because of the tensile stress release as our speculation. Fig. 3 summarizes the values of full width half maximum (FWHM) for Raman spectra in the E_{2g}¹ and A_{1g} mode peaks. The FWHM values decrease

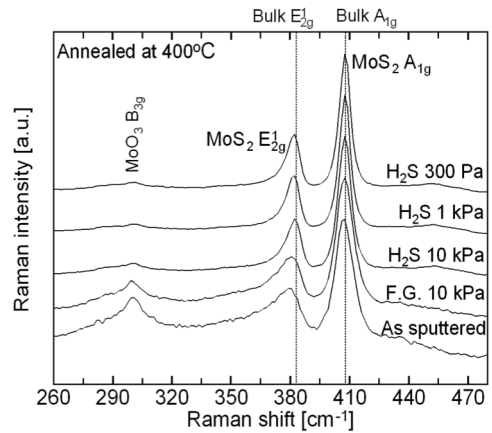


FIGURE 1. Raman spectra for as-sputtered and annealed MoS₂ films depending on annealing gas and pressure.

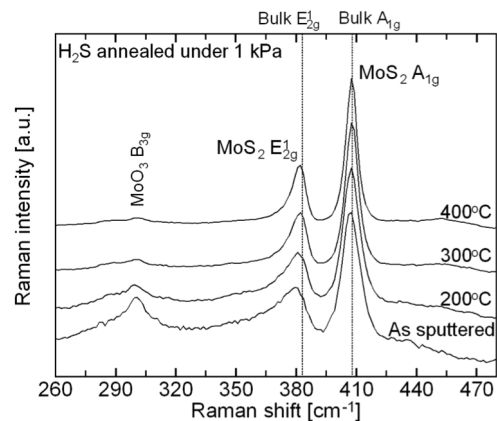


FIGURE 2. Raman spectra for as-sputtered and H₂S-annealed MoS₂ films depending on annealing temperature.

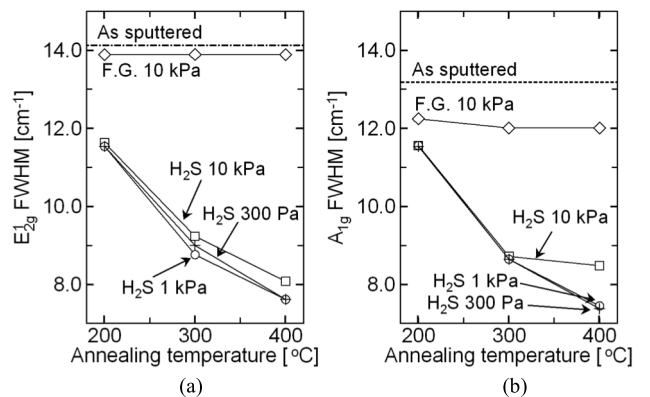


FIGURE 3. FWHM values for sputtered-MoS₂ Raman spectra in (a) E_{2g}¹ and (b) A_{1g} mode peaks.

with an increase in the annealing temperature. Reducing the annealing pressure is effective to reduce the FWHM values except 10 kPa. As a result, the FWHM values of E_{2g}¹ and A_{1g} remarkably decrease from 14.1 to 7.6 cm⁻¹ and from 13.2 to 7.4 cm⁻¹ when optimal H₂S annealing is used. It

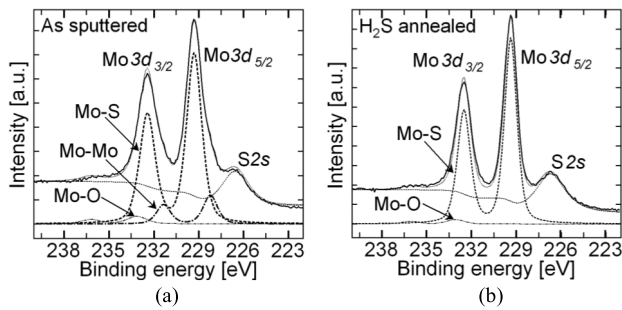


FIGURE 4. XPS spectra of molybdenum 3d for (a) as-sputtered and (b) H₂S-annealed MoS₂ films at 400°C under 1 kPa.

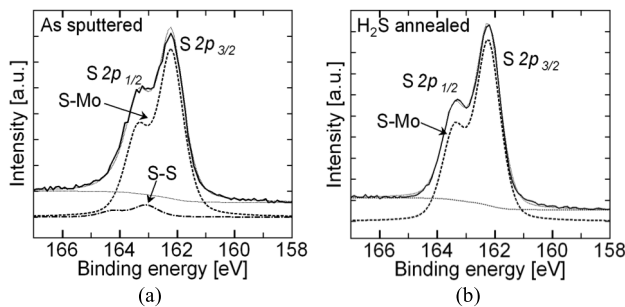


FIGURE 5. XPS spectra of sulfur 2p for (a) as-sputtered and (b) H₂S-annealed MoS₂ films at 400°C under 1 kPa.

is speculated that all of these results are obtained because of the successful compensation of sulfur into sulfur defects using the H₂S annealing in sputtered-MoS₂ film.

Figs. 4(a) and (b) show the XPS spectra of Mo 3d for the as-sputtered and H₂S-annealed MoS₂ films. To analyze the Mo 3d components, the peaks were fitted with a pseudo-Voigt function. Although an as-sputtered MoS₂ film has the Mo–S, Mo–Mo, and Mo–O components [29]–[31], a Mo–Mo component is not observed in the H₂S-annealed MoS₂ film indicating successful sulfurization of residual molybdenum by H₂S annealing. However, the MoS₂ film still has a slight Mo–O component even after H₂S annealing. On the other hand, Figs. 5(a) and (b) show the XPS spectra of S 2p. The S–S component is observed within the MoS₂ film after the sputtering process. In contrast, the S–S peak is not observed after H₂S annealing. This agrees with a previous report in which residual sulfur in the as-sputtered MoS₂ film reacted with sulfur defects when F.G. annealing is carried out at 400°C [36]. These results in this paragraph agree with the results of Raman spectra as shown in above.

The S/Mo ratio was also investigated to estimate the state of chemical bonds before and after the H₂S annealing process. We calculated the area of each peak of the Mo–S, Mo–Mo, and S–Mo components. The results showed that the S/Mo ratio improved from 1.47 to 1.90 by H₂S annealing.

A cross-sectional high-angle-annular dark field (HAADF) STEM image in Fig. 6 shows overall features of the H₂S-annealed MoS₂ film at 400°C under 300 Pa. It is confirmed that a two-dimensionally layered MoS₂ film is successfully

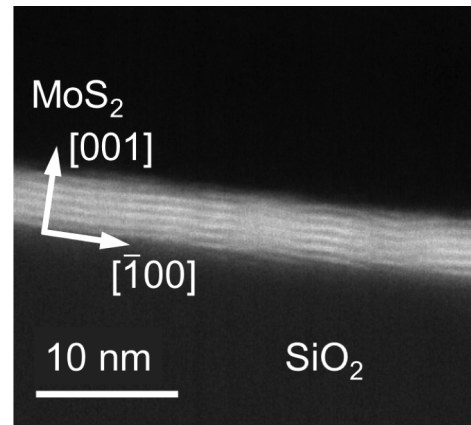


FIGURE 6. Cross-sectional STEM image for MoS₂ film annealed in H₂S gas at 400°C under 300 Pa.

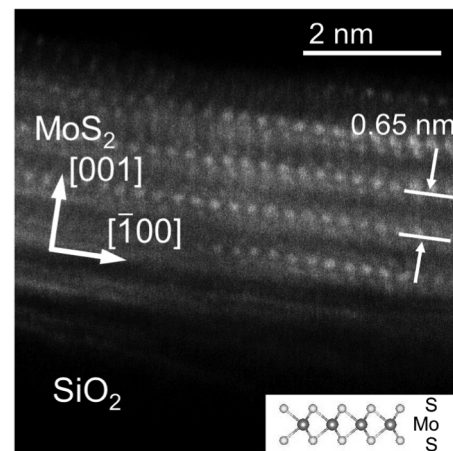


FIGURE 7. High-resolution image from [010] direction of H₂S-annealed MoS₂ film at 400°C under 300 Pa and schematic image of MoS₂.

formed with uniform thickness. Here, the significant thickness change between before and after H₂S anneal process was not observed yet, however it is needed to confirm carefully. Moreover, a grain size is approximately 10 nm, which is smaller than what we had expected. Fig. 7 shows a high-resolution HAADF-STEM image of the same sample. It is successfully observed a triangle shape of the Mo–S atomic arrangement within a 5-layer MoS₂ film having an interlayer distance of 0.65 nm. Therefore we considered that an appropriate MoS₂ film was obtained using the H₂S annealing.

To determine the electrical characteristics, the carrier densities of the MoS₂ film are firstly shown in Fig. 8. The carrier density in n-type decreases with an increase in the annealing temperature. It is considered that this is because of the compensation of sulfur defects. A carrier density of $9.3 \times 10^{15} \text{ cm}^{-3}$ is achieved even at 400°C, which is significantly lower compared to reported value with 10^{20} cm^{-3} for an exfoliated-MoS₂ film [40], [41]. As shown in Fig. 9, the Hall-effect mobility of electrons is enhanced by H₂S annealing at up to 300°C, even though

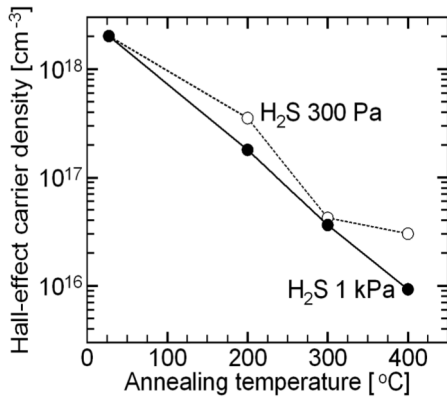


FIGURE 8. Carrier density by Hall-effect measurement depending on annealing temperature.

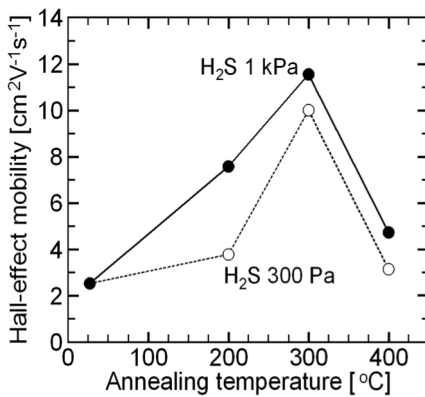


FIGURE 9. Hall-effect mobility depending on annealing temperature.

carrier density continuously decreases up to 400°C. Here, H₂S gas is decomposed over 400°C; this might be one of the reasons that mobility decreases at 400°C. Eventually, the H₂S annealing remarkably achieves the Hall-effect mobility of up to 12 cm²V⁻¹s⁻¹ and the carrier density of 3.5×10^{17} cm⁻³ at 300°C. This value of carrier density is still low enough to realize a normally-off accumulation-mode MOSFET with the MoS₂ channel.

IV. CONCLUSION

High-quality MoS₂ films were formed by sputtering at 360°C and by performing H₂S annealing at 300°C. The sulfur defects of the sputtered MoS₂ film were effectively compensated by H₂S annealing, and MoS₂ films with good crystallinity in Raman spectra and a higher S/Mo ratio of 1.90 were obtained. Eventually from the Hall-effect measurement, carrier density reduction down to 3.5×10^{17} cm⁻³ and mobility improvement up to 12 cm²V⁻¹s⁻¹ were simultaneously achieved. These results show that sputtering and H₂S annealing is applicable to obtain high-quality MoS₂ film for 3D-monolithic IC applications.

REFERENCES

[1] A. Splendiani *et al.*, "Emerging photoluminescence in monolayer MoS₂," *Nano Lett.*, vol. 10, no. 4, pp. 1271–1275, 2010.

[2] K. F. Mak, C. Lee, J. Hone, J. Shan, and T. F. Heinz, "Atomically thin MoS₂: A new direct-gap semiconductor," *Phys. Rev. Lett.*, vol. 105, no. 13, pp. 2–5, 2010.

[3] S. Das, H.-Y. Chen, A. V. Penumatcha, and J. Appenzeller, "High performance multilayer MoS₂ transistors with scandium contacts," *Nano Lett.*, vol. 13, no. 1, pp. 100–105, 2012.

[4] B. Radisavljevic, A. Radenovic, J. Brivio, V. Giacometti, and A. Kis, "Single-layer MoS₂ transistors," *Nat. Nanotechnol.*, vol. 6, no. 3, pp. 147–150, 2011.

[5] H. Wang *et al.*, "Integrated circuits based on bilayer MoS₂ transistors," *Nano Lett.*, vol. 12, no. 9, pp. 4674–4680, 2012.

[6] M. Poljak, V. Jovanović, D. Grgec, and T. Suligoj, "Assessment of electron mobility in ultrathin-body InGaAs-on-insulator MOSFETs using physics-based modeling," *IEEE Trans. Electron Devices*, vol. 59, no. 6, pp. 1636–1643, Jun. 2012.

[7] K. Uchida *et al.*, "Experimental study on carrier transport mechanism in ultrathin-body SOI n- and p-MOSFETs with SOI thickness less than 5 nm," in *Proc. Int. Electron Devices Meeting*, San Francisco, CA, USA, 2002, pp. 47–50.

[8] S. Krivec, M. Poljak, and T. Suligoj, "Electron mobility in ultrathin InGaAs channels: Impact of surface orientation and different gate oxide materials," *Solid-State Electron.*, vol. 115, pp. 109–119, Jan. 2016.

[9] J. N. Coleman *et al.*, "Two-dimensional nanosheets produced by liquid exfoliation of layered materials," *Science*, vol. 331, no. 6017, pp. 568–571, 2011.

[10] L. Yu *et al.*, "MoS₂ FET fabrication and modeling for large-scale flexible electronics," in *Proc. Symp. VLSI Technol.*, Kyoto, Japan, 2015, pp. T144–T145.

[11] A. Nourbakhsh *et al.*, "15-Nm channel length MoS₂ FETs with single- and double-gate structures," in *Proc. Symp. VLSI Technol.*, Kyoto, Japan, 2015, pp. T28–T29.

[12] L. Yu *et al.*, "Enhancement-mode single-layer CVD MoS₂ FET technology for digital electronics," in *Proc. IEDM*, Washington, DC, USA, 2015, pp. 32.3.1–32.3.4.

[13] Y. H. Lee *et al.*, "Synthesis of large-area MoS₂ atomic layers with chemical vapor deposition," *Adv. Mater.*, vol. 24, no. 17, pp. 2320–2325, 2012.

[14] D. Krasnozhan, S. Dutta, C. Nyffeler, Y. Leblebici, and A. Kis, "High-frequency, scaled MoS₂ transistors," in *Proc. IEDM*, Washington, DC, USA, 2015, pp. 27.4.1–27.4.4.

[15] Y. Kim, H. Bark, G. H. Ryu, Z. Lee, and C. Lee, "Wafer-scale monolayer MoS₂ grown by chemical vapor deposition using a reaction of MoO₃ and H₂S," *J. Phys. Condens. Matter*, vol. 28, no. 18, 2016, Art. no. 184002.

[16] D. Dumcenco *et al.*, "Large-area MoS₂ grown using H₂S as the sulphur source," *2D Mater.*, vol. 2, no. 4, 2015, Art. no. 44005.

[17] P. Batude *et al.*, "3DVLSI with CoolCube process: An alternative path to scaling," in *Proc. Symp. VLSI Technol.*, Kyoto, Japan, 2015, pp. T48–T49.

[18] P. Batude *et al.*, "3-D sequential integration: A key enabling technology for heterogeneous co-integration of new function with CMOS," *IEEE Trans. Emerg. Sel. Topics Circuits Syst.*, vol. 2, no. 4, pp. 714–722, Dec. 2012.

[19] D. H. Kwon, Z. Jin, S. Shin, W.-S. Lee, and Y.-S. Min, "A comprehensive study on atomic layer deposition of molybdenum sulfide for electrochemical hydrogen evolution," *Nanoscale*, vol. 8, pp. 7180–7188, Feb. 2016.

[20] S. Shin, Z. Jin, D. H. Kwon, R. Bose, and Y. S. Min, "High turnover frequency of hydrogen evolution reaction on amorphous MoS₂ thin film directly grown by atomic layer deposition," *Langmuir*, vol. 31, no. 3, pp. 1196–1202, 2015.

[21] Z. Jin, S. Shin, D. H. Kwon, S.-J. Han, and Y.-S. Min, "Novel chemical route for atomic layer deposition of MoS₂ thin film on SiO₂/Si substrate," *Nanoscale*, vol. 6, no. 23, pp. 14453–14458, 2014.

[22] L. K. Tan *et al.*, "Atomic layer deposition of a MoS₂ film," *Nanoscale*, vol. 6, no. 8, pp. 10584–10588, 2014.

[23] R. Browning *et al.*, "Atomic layer deposition of MoS₂ thin films," *Mater. Res. Express*, vol. 2, no. 3, 2015, Art. no. 35006.

[24] A. Valdivia, D. J. Tweet, and J. F. Conley, "Atomic layer deposition of two dimensional MoS₂ on 150 mm substrates," *J. Vac. Sci. Technol. A Vac. Surfaces Film.*, vol. 34, no. 2, 2016, Art. no. 21515.

[25] Y. Kim *et al.*, "Self-limiting layer synthesis of transition metal dichalcogenides," *Sci. Rep.*, vol. 6, Jan. 2016, Art. no. 18754.

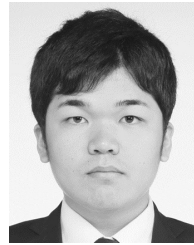
- [26] M. Mattinen *et al.*, "Atomic layer deposition of crystalline MoS₂ thin films: New molybdenum precursor for low-temperature film growth," *Adv. Mater. Interfaces*, vol. 4, Mar. 2017, Art. no. 1700123.
- [27] J. Tao *et al.*, "Growth of wafer-scale MoS₂ monolayer by magnetron sputtering," *Nanoscale*, vol. 7, pp. 2497–2503, Jan. 2015.
- [28] S. Hirano *et al.*, "Crystallinity improvement using migration-enhancement methods for sputtered-MoS₂ films," in *Proc. 1st Electron Devices Technol. Manuf. (EDTM)*, 2017, pp. 234–235.
- [29] S. Ishihara *et al.*, "Large scale uniformity of sputtering deposited single- and few-layer MoS₂ investigated by XPS multipoint measurements and histogram analysis of optical contrast," *ECS J. Solid State Sci. Technol.*, vol. 5, no. 11, pp. 3012–3015, 2016.
- [30] S. Ishihara *et al.*, "Improving crystalline quality of sputtering-deposited MoS₂ thin film by postdeposition sulfurization annealing using (t-C₄H₉)₂S₂," *Jpn. J. Appl. Phys.*, vol. 55, Mar. 2016, Art. no. 04EJ07.
- [31] S. Ishihara *et al.*, "Properties of single-layer MoS₂ film fabricated by combination of sputtering deposition and post deposition sulfurization annealing using (t-C₄H₉)₂S₂," *Jpn. J. Appl. Phys.*, vol. 55, Apr. 2016, Art. no. 06GF01.
- [32] K. Matsuura *et al.*, "Sulfurization in sulfur vapor for sputtered-MoS₂ film," in *Proc. 47th SISC*, 3.6, 2016.
- [33] T. Ohashi *et al.*, "Quantitative relationship between sputter-deposited-MoS₂ properties and underlying-SiO₂ surface roughness," *Appl. Phys. Exp.*, vol. 10, no. 4, 2017, Art. no. 41202.
- [34] T. Ohashi *et al.*, "Multi-layered MoS₂ film formed by high-temperature sputtering for enhancement-mode nMOSFETs," *Jpn. J. Appl. Phys.*, vol. 54, no. 4, 2015, Art. no. 04DN08.
- [35] J. Shimizu *et al.*, "Low-carrier density sputtered-MoS₂ film by H₂S annealing for normally-off accumulation-mode FET," in *Proc. 1st EDTM*, 2017, pp. 222–223.
- [36] J. Shimizu *et al.*, "High-mobility and low-carrier-density sputtered MoS₂ film formed by introducing residual sulfur during low-temperature in 3%-H₂ annealing for three-dimensional ICs," *Jpn. J. Appl. Phys.*, vol. 56, Mar. 2017, Art. no. 04CP06.
- [37] S. Tongay *et al.*, "Defects activated photoluminescence in two-dimensional semiconductors: Interplay between bound, charged, and free excitons," *Sci. Rep.*, vol. 3, p. 2657, Sep. 2013.
- [38] B. C. Windom, W. G. Sawyer, and D. W. Hahn, "A Raman spectroscopic study of MoS₂ and MoO₃: Applications to tribological systems," *Tribol. Lett.*, vol. 42, no. 3, pp. 301–310, Jun. 2011.
- [39] B. H. Kim *et al.*, "Effect of Sulphur vacancy on geometric and electronic structure of MoS₂ induced by molecular hydrogen treatment at room temperature," *RSC Adv.*, vol. 3, no. 40, Aug. 2013, Art. no. 18424.
- [40] B. Radisavljevic and A. Kis, "Mobility engineering and a metal-insulator transition in monolayer MoS₂," *Nat. Mater.*, vol. 12, no. 9, pp. 815–820, 2013.
- [41] Y. Zhang, J. Ye, Y. Matsuhashi, and Y. Iwasa, "Ambipolar MoS₂ thin flake transistors," *Nano Lett.*, vol. 12, no. 3, pp. 1136–1140, 2012.



JUN'ICHI SHIMIZU received the B.E. and M.E. degrees in electrical engineering from the Tokyo Institute of Technology, Japan, in 2016 and 2018, respectively.
He is currently with Daikin Industries, Ltd., Osaka, Japan.



TAKUMI OHASHI received the B.E., M.E., and Ph.D. degrees in electrical engineering from the Tokyo Institute of Technology, Tokyo, Japan, in 2014, 2016, and 2018, respectively, where he is currently a Faculty Member.



KENTARO MATSUURA received the B.E. and M.E. degrees in electrical engineering from the Tokyo Institute of Technology, Yokohama, Japan, in 2015 and 2017, respectively, where he is currently pursuing the Doctoral degree.



IRIYA MUNETA (M'16) received the Bachelor of Engineering and Master of Engineering degrees and the Ph.D. degree in engineering from the University of Tokyo in 2009, 2011, and 2014, respectively, where he was a Post-Doctoral Researcher for two years and he thoroughly investigated molecular beam epitaxy, materials science, and electronic devices of ferromagnetic semiconductors. In 2016, he joined the Tokyo Institute of Technology, where he is currently an Assistant Professor. His current research is focused on 2-D materials and transition-metal di-chalcogenides, especially on deposition of thin films, materials science, and device integration of them.



KUNIYUKI KAKUSHIMA (M'99) received the B.S., M.S., and Ph.D. degrees in electrical engineering from the University of Tokyo, Tokyo, Japan, in 1999, 2001, and 2004, respectively.
He is currently an Associate Professor with the Tokyo Institute of Technology, Yokohama, Japan.



KAZUO TSUTSUI (M'02–SM'07) received the B.E., M.E., and Ph.D. degrees in electrical engineering from the Tokyo Institute of Technology, Yokohama, Japan, in 1981, 1983, and 1986, respectively.
He is currently with the Tokyo Institute of Technology.



NOBUYUKI IKARASHI received the Ph.D. degree in science from the Tokyo Institute of Technology, Tokyo, Japan, in 1999.
He is currently a Professor with Institute of Materials and Systems for Sustainability, Nagoya University, Nagoya, Japan.
Dr. Ikarashi's research interest includes the physics and materials science of advanced semiconductor devices.



HITOSHI WAKABAYASHI (M'00) received the M.E. and Ph.D. degrees in electrical engineering from the Tokyo Institute of Technology, Yokohama, Japan, in 1993 and 2003, respectively.
He was with NEC Corporation from 1993 to 2006, Massachusetts Institute of Technology from 2000 to 2001, and Sony Corporation from 2006 to 2012. Since 2013, he has been with the Tokyo Institute of Technology as a Faculty Member.